Portable 3D/4D Ultrasound Diagnostic Imaging System

Stergios Stergiopoulos, Ph.D.
Defence R&D Canada – Toronto
1133 Sheppard Ave West, P.O. Box 2000
Toronto, Ontario M3K 2C9
CANADA

Stergios.Stergiopoulos@drdc-rddc.gc.ca

Pang Shek, Ph.D.
Defence R&D Canada – Toronto
1133 Sheppard Ave West, P.O. Box 2000
Toronto, Ontario M3K 2C9
CANADA

Pang.Shek@drdc-rddc.gc.ca

ABSTRACT

The rapid diagnosis of invisible internal injury in an austere and hostile front-line operational environment remains a challenge for (Canadian Forces) medical and search and rescue personnel. The availability of a portable 4D-ultrasound imaging system with a single probe, providing high image resolution and deep penetration, is considered by (civilian) medical practitioners and their military health services counterparts as exceedingly helpful, if not essential in supporting triage and medical decisions to save lives. However, portable and easy-to-use 4D non-invasive medical imaging systems are not yet commercially available, primarily because of unresolved major technological and engineering challenges. Available portable ultrasound systems only provide 2D images, requiring a medical professional to mentally integrate multiple images to develop a 3D impression of the scanned objects. This practice is time-consuming, inefficient, and requires a highly skilled operator to administer the scanning procedure. Defence R&D Canada (DRDC) is developing a Portable 3D/4D Ultrasound Diagnostic Imaging System (PUDIS) to address the above-mentioned challenges. Our proposed approach to address the conventional 2D ultrasound imaging limitations is to implement 3D adaptive beamformers in portable 4D ultrasound imaging systems, that can improve image resolution for low frequency planar array probes. Along these lines, DRDC has allocated significant investments to develop an advanced, fully-digital 4D (3D-spatial + 1D-temporal) ultrasound imaging technology for improving image resolution and facilitating auto-diagnostic applications to detect non-visible internal injuries, based on the volumetric imaging outputs provided by a 4D ultrasound imaging system that includes:

- *A 32x32 sensor planar array ultrasound probe with a fully digital data acquisition peripheral;*

- *A portable ultrasound computing architecture consisting of a cluster of DSPs and CPUs;*

- *Adaptive 3D beamforming algorithms with volumetric visualization, including fusion and automated segmentation capabilities; and*

- *The implementation of a decision-support process to provide automated diagnostic capabilities for non-invasively detecting internal injuries and facilitate image guided surgery.*

1.0   INTRODUCTION

The fully digital 3-Dimensional (3D)/ (4D: 3D + time) Ultrasound System Technology, presented in this paper, consists of a set of adaptive ultrasound beamformers [1-4] that have been discussed in detail in [3,6]. The aim with this signal processing structure is to address the fundamental image resolution problems of current ultrasound systems [6-8] and to provide suggestions for its implementation into existing 2D and/or 3D ultrasound systems as well as develop a complete stand-alone 3D ultrasound solution. This development has

Report Documentation Page		Form Approved OMB No. 0704-0188

1. REPORT DATE **APR 2010**	2. REPORT TYPE **N/A**	3. DATES COVERED **-**

4. TITLE AND SUBTITLE **Portable 3D/4D Ultrasound Diagnostic Imaging System**		5a. CONTRACT NUMBER
		5b. GRANT NUMBER
		5c. PROGRAM ELEMENT NUMBER
6. AUTHOR(S)		5d. PROJECT NUMBER
		5e. TASK NUMBER
		5f. WORK UNIT NUMBER
7. PERFORMING ORGANIZATION NAME(S) AND ADDRESS(ES) **Defence R&D Canada Toronto 1133 Sheppard Ave West, P.O. Box 2000 Toronto, Ontario M3K 2C9 CANADA**		8. PERFORMING ORGANIZATION REPORT NUMBER
9. SPONSORING/MONITORING AGENCY NAME(S) AND ADDRESS(ES)		10. SPONSOR/MONITOR'S ACRONYM(S)
		11. SPONSOR/MONITOR'S REPORT NUMBER(S)

12. DISTRIBUTION/AVAILABILITY STATEMENT **Approved for public release, distribution unlimited**

13. SUPPLEMENTARY NOTES **See also ADA564622. Use of Advanced Technologies and New Procedures in Medical Field Operations (Utilisation de technologies avancees et de procedures nouvelles dans les operations sanitaires). RTO-MP-HFM-182**

14. ABSTRACT

The rapid diagnosis of invisible internal injury in an austere and hostile front-line operational environment remains a challenge for (Canadian Forces) medical and search and rescue personnel. The availability of a portable 4D-ultrasound imaging system with a single probe, providing high image resolution and deep penetration, is considered by (civilian) medical practitioners and their military health services counterparts as exceedingly helpful, if not essential in supporting triage and medical decisions to save lives. However, portable and easy-to-use 4D non-invasive medical imaging systems are not yet commercially available, primarily because of unresolved major technological and engineering challenges. Available portable ultrasound systems only provide 2D images, requiring a medical professional to mentally integrate multiple images to develop a 3D impression of the scanned objects. This practice is time-consuming, inefficient, and requires a highly skilled operator to administer the scanning procedure. Defence R&D Canada (DRDC) is developing a Portable 3D/4D Ultrasound Diagnostic Imaging System (PUDIS) to address the above-mentioned challenges. Our proposed approach to address the conventional 2D ultrasound imaging limitations is to implement 3D adaptive beamformers in portable 4D ultrasound imaging systems, that can improve image resolution for low frequency planar array probes. Along these lines, DRDC has allocated significant investments to develop an advanced, fully-digital 4D (3D-spatial + 1D-temporal) ultrasound imaging technology for improving image resolution and facilitating auto-diagnostic applications to detect non-visible internal injuries, based on the volumetric imaging outputs provided by a 4D ultrasound imaging system that includes: A 32x32 sensor planar array ultrasound probe with a fully digital data acquisition peripheral; A portable ultrasound computing architecture consisting of a cluster of DSPs and CPUs; Adaptive 3D beamforming algorithms with volumetric visualization, including fusion and automated segmentation capabilities; and The implementation of a decision-support process to provide automated diagnostic capabilities for non-invasively detecting internal injuries and facilitate image guided surgery.

15. SUBJECT TERMS

16. SECURITY CLASSIFICATION OF:			17. LIMITATION OF ABSTRACT	18. NUMBER OF PAGES	19a. NAME OF RESPONSIBLE PERSON
a. REPORT **unclassified**	b. ABSTRACT **unclassified**	c. THIS PAGE **unclassified**	**SAR**	**22**	

To fully exploit the advantages of the present fully digital adaptive ultrasound technology, its implementation in a commercial ultrasound system requires that the system has a fully digital design configuration consisting of A/DC and D/AC peripherals that have the capability to digitize the ultrasound probe time series, to optimally shape the transmitted ultrasound pulses through a D/A peripheral and to integrate linear and/or planar phase array ultrasound probes.

Thus, the digital ultrasound 3D beamforming technology of this paper, can replace the conventional (i.e. time delay) beamforming structure of ultrasound systems with an adaptive beamforming processing configuration. The results of this development [1,2,6] demonstrate that adaptive beamformers improve significantly (at very low cost) the image resolution capabilities of an ultrasound imaging system by providing a performance improvement equivalent to a deployed ultrasound probe with double aperture size . Furthermore, the portability and the low cost characteristics of the present 3D adaptive ultrasound technology can offer the options to medical practitioners and family physicians to have access of diagnostic imaging systems readily available on a daily basis. As a result, a digital PC-based ultrasound technology can adjust the signal processing configuration of ultrasound devices to move them away from the traditional hardware and implementation software requirements and to be able to accommodate the processing requirements of the "traditional" linear array 2D scans as well as the advanced matrix-arrays performing volumetric scans.

In summary, a digital PC-based ultrasound imaging technology can provide flexible cost-to-image quality adjustments. The resulting systems can be upgraded on a continuous base at very low cost by means of software and hardware improvements by exploiting the continuous upgrades and CPU performance improvements of the PC architectures.

Thus, to maintain a reasonable image quality, a large number of detector elements are required, and the computational load is directly related to the size of 2-D array (i.e. planar array ultrasound probe) used to acquire the RF time series for beamforming.

The ability to image volumes, instead of slices is the motivation for using a 3-D beamformer. Currently to generate an ultrasound volume, a number of slices are collected. These slices are then used to synthesize a 3D volume. Another approach is to use 2-D array probes to generate 3D ultrasound volumes, but to counter the increased processing load brought on by the 2-D probe the resolution in one of the directions (x or y) is compromised.

As stated above, the core of the system design presented here is the efficient implementation of 3D beamforming that greatly simplifies the beamformer processing. This implementation makes it possible to map the processing onto a parallel computing architecture like the multi-node cluster described later. The beamforming algorithm is implemented on the processing cluster along with a versatile data control unit that controls all signal transmission and reception form the complete 3D/4D Ultrasound system.

An additional complication is that in ultrasound imaging systems the angular resolution provided by conventional beamformers is determined by the length of the aperture L, and by the frequency of the received signals [1,2,6]. Since the operating frequency is usually fixed, only the aperture length can be eventually increased by a higher number of elements, thus leading to more complex hardware and software implementations. The alternative is to employ an adaptive beamforming method. Adaptive beamformers are designed to maximize signal detection, while minimizing the beam-width, and suppressing the side-lobes

[1,2,3]. The convergence time of the specific method adopted allows for real-time imaging [6]. The method uses a combination of the Sub-Aperture pre-processing scheme [4] and a space-time statistic [3,4] to reduce the degrees of freedom required by the algorithm.

2.0   THE BEAMFORMING PROCESS IN 3D/4D ULTRASOUND SYSTEMS

2.1   Conventional 3D Beamformer

Consider the beamforming process for an N x M detector array with K time samples collected, the data collected is given by

$$x_{nm}(t_k), n = 1, \ldots N, m = 1 \ldots M, k = 1 \ldots K. \tag{1}$$

The time domain focused beamformer outputs implemented in the frequency domain, the beam-time series obtained from the beamformer, $b(t_j, A, B, R) = IFFT\big[B(f_i, A, B, R)\big]$, is given by (2), where the parameters are defined in Figure 1.

$$B(f_i, A, B, R) = \sum_{n=0}^{N-1} \sum_{m=0}^{M-1} X_{nm}(f_i) \cdot S_{nm}(f_i, A, B, R), \tag{2}$$

where $X_{nm}(f_i) = FFT\big[x_{nm}(t_j)\big]$ and the steering vector $S_{nm}(f_i, A, B, R) = \exp\big(j2\pi f_i \tau_{nm}(A, B, R)\big)$.

The inter-element time delays are defined by (3).

$$\tau_{m,n}(A, B, R) = \frac{\sqrt{R^2 + x_m^2 + y_n^2 - 2x_m \cos A - 2y_n \cos B} - R}{c} \tag{3}$$

where element nm is located at position (x_m, y_n).

Equation 3 indicates that for each beam *(A,B)* and focal depth R there needs to be *MxN* complex steering vectors computed for each frequency bin of interest. Furthermore each set of steering vectors $S_{nm}(f_j, A, B, R)$ is unique, with each of the four function variable independent and not separable. Because of this independence, it is not possible to decompose this beamformer in an efficient manner [2,4].
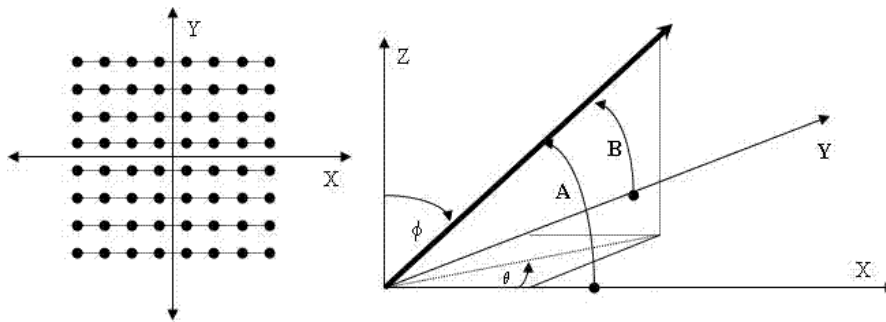

Figure 1: Definition of Parameters.

The approach that follows presents an alternative beamformer that is an approximation to the beamformer in (2) [1,2,3]. This implementation allows the beamforming equation to be divided, and hence decomposed, which in turn allows for it to be easily implemented on a parallel architecture. The difference between this 3D implementation and the efficient beamformer implementation is shown in (2) and (4), where (2) is approximated (4), resulting in a simplified 2-stage implementation. For plane wave arrivals, i.e. $R \rightarrow \infty$, (4) can be directly derived from (2) and the derivation is exact. For (x_m, y_n) the exact beamforming delay τ_{nm} is approximated to:

$$\tau_{nm}(A,B,R) = \frac{\sqrt{R^2 + x_m^2 - 2x_m R\cos A} - R}{c}$$
$$+ \frac{\sqrt{R^2 + y_n^2 - 2y_n R\cos B} - R}{c} \quad . \tag{4}$$

The decomposition of the 3D beamforming into two linear steps is expressed as follows:

$$B(f_i, A, B, R) = \sum_{n=0}^{N-1} S_n(f_i, B, R) \cdot \left[\sum_{m=0}^{M-1} X_{nm}(f_i) \cdot S_m(f_i, A, R) \right]$$

with the two separated steering vectors expressed as:

$$S_m(f_i, A, R) = \exp\left\{ j2\pi f_i \left(\frac{\sqrt{R^2 + x_m^2 - 2x_m R\cos A} - R}{c} \right) \right\}$$

$$S_n(f_i, B, R) = \exp\left\{ j2\pi f_i \left(\frac{\sqrt{R^2 + y_n^2 - 2y_n R\cos B} - R}{c} \right) \right\} \quad . \tag{5}$$

The summation in square brackets is equal to a line array beamformer along the X-axis. This term is a vector which can be denoted as $B_n(f_i, A, R)$. This can then be rewritten as follows:

$$B(f_i, A, B, R) = \sum_{n=0}^{N-1} B_n(f_i, A, R) \cdot S_n(f_i, B, R) \tag{6}$$

This expression is equal to a linear beamforming along the Y-axis, with $B_n(f_i, A, R)$ as input. This 2 stage implementation is easily parallelized and implemented on a multi-node system. In this approximate implementation, the error introduced at angles A and B close to broadside is negligible. Side by side comparisons show that there is no degradation in image quality over the exact implementation for this application.

2.2 Adaptive Beamforming

The beamforming method presented in this paper is based on the class of Linear Constrained Minimum Variance (LCMV) adaptive beamformers [1,2,3,4].

Consider a linear phased array of N transducers, with θ_0 steering angle. The optimum beam-steering vector, $\overline{W}(f_i, \theta_0)$, is solution of a constrained minimization problem [4]. The cost function is:

$$\sigma_{MV}^2(f_i, \theta_0) = \overline{W}^H(f_i, \theta_0) \cdot \Phi(f_0, \theta_0) \cdot \overline{W}(f_i, \theta_0) \tag{7}$$

where ^{H} denotes the complex conjugate transpose. $\Phi(f_0, \theta_0)$ is the Steered Covariance Matrix (STCM): it is a space-time statistic, exploiting the signals' characteristics both in frequency and in time [3,4]. For a band of width Δf centred at f_0, the STCM for the bins at f_0 and the steering angle θ_0 is defined as:

$$\Phi(f_0, \theta_0) = \sum_{f_i = f_0 - \Delta f/2}^{f_0 + \Delta f/2} \left[\overline{X}(f_i) \cdot \overline{D}(f_i, \theta_0)\right] \cdot \left[\overline{X}(f_i) \cdot \overline{D}(f_i, \theta_0)\right]^H \tag{8}$$

where $\cdot$ denotes element-by-element multiplication. $\overline{X}(f_i)$ is an Nx1 vector, containing for each nth transducer of the array the corresponding sample $X_n(f_i)$, as defined by (1) and $\overline{D}(f_i, \theta_0)$ is the conventional steering vector for a line array, which is different than that defined by Eqs. (2) & (5). The constraint to be fulfilled by the steering vector is:

$$\overline{W}^H(f_i, \theta_0) \cdot \overline{D}(f_i, \theta_0) = 1 \tag{9}$$

The method based on the STCM is called Steered Minimum Variance algorithm (STMV).

Assuming stationarity across the frequency bins of a band Δf, then for each frequency bin in Δf the STCM may be considered to be approximately the same as the narrowband estimate $\Phi(f_0, \theta_0)$ for the centre frequency f_0 of the band Δf. For each bin f_i in Δf, the adaptive coefficients are then given by the following expression:

$$\overline{W}(f_i, \theta_0) = \frac{\Phi(f_0, \theta_0)^{-1} \cdot \overline{D}(f_i, \theta_0)}{\overline{D}^H(f_i, \theta_0) \cdot \Phi(f_0, \theta_0)^{-1} \cdot \overline{D}(f_i, \theta_0)} \tag{10}$$

This method is called Steered Minimum Variance Narrowband Algorithm [1-3]. The adaptive beam is then obtained as:

$$B(f_i, \theta_0) = \overline{W}^H(f_i, \theta_0) \cdot \overline{X}(f_i) \tag{11}$$

It has been shown [3] that for broad-band sources this method achieves lower convergence times than other adaptive beamformers. The reader is referred to [1-4] for further information on near-instantaneous convergence beamforming.

3.0 IMPLEMENTATION

The hardware components designed to complement the efficient beamformer defined in Section 2.0, is a data acquisition unit that supports a 16 x 16 planar array probe, and the scaleable multi-node cluster. The implementations of the individual functional components of the system are described in this section.

3.1   Transmit Functionality

The philosophy of the energy transmission module is to illuminate the entire volume of interest with a few firings. This is shown in Figure 2. Here the volume is illuminated in 3 x 3 sectors, meaning a total of 9 firings. The transmitted signals are all broadband FM (chirp) signals. They are fired with inter-element delays to allow the transmitted energy to be focused at specific regions in space, e.g. the space highlighted by the square shaded areas of Figure 2. The energy transmission is done through the 6 x 6 elements at the center of the array. The transmit patterns are loaded into the memory of the data acquisition unit and delivered to the probe via the D/A portion of the unit when a trigger signal is received.
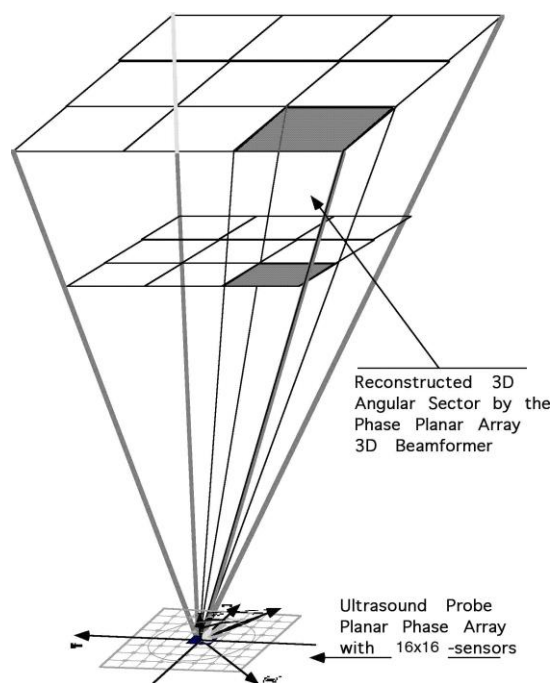

Reconstructed 3D Angular Sector by the Phase Planar Array 3D Beamformer

Ultrasound Probe Planar Phase Array with 16x16 -sensors

Figure 2: The Phased Array Transmit Function of the Planar Array Probe.

In addition, FM pulses that occupy different non-overlapping frequency regimes may be coded together to illuminate different focal depths with a single firing. This means that it can be arranged so that one frequency regime can focus and illuminate the lower shaded square, and a second frequency regime the upper shaded square in Figure 2.

The use of fewer beams to illuminate the volume of interest however leads to a non-uniform energy distribution in space. This requires the application of a linearization function to correct for this type of non-uniformity. A correction function is derived from the illuminating beam shapes and is used later for linearization of the results of the beamformer. An example of a linearization function is shown in Figure 3. This figure shows the correction function that would be applied to the output for a 4 x 4 sector illumination.
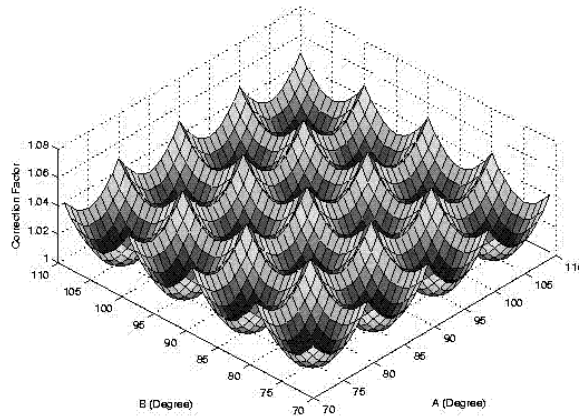
Figure 3: Correction function for 4 x 4 sectors illumination pattern.

3.2 The Beamformer

The 2-stage beamformer described by Equations (4) and (5) is implemented as shown in Figure 4 [3]. The beamforming process is a two stage process where the rows are treated as line arrays and beamformed accordingly. The results of this first stage of beamforming are again treated as line arrays and beamformed. Figure 4 outlines this process. Each row of the array is sent to a line array beamformer, which includes transforming the signals to the frequency domain through the FFT, applying a filter and steering the azimuth beams. The azimuth beams are then grouped, and for a fixed azimuth beam, the results of all of the rows are then sent to the second stage of line array beamforming. This second stage includes steering the elevation beams and transferring the results back   to the time domain. For every azimuth beam a series of elevation beams are created [1,2,3,6].
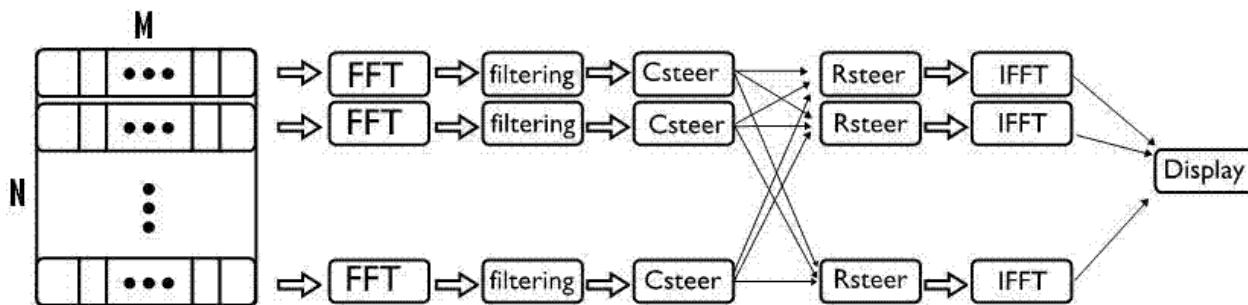

Figure 4: Block Diagram showing the 2 Stage Implementation of the 3D beamformer.

The implementation shown in Figure 4 is easily realizable on a parallel system. The first stage beamforming is distributed to the computing nodes. In the simplest sense each row of data is distributed to a separate node and processed. The results are then regrouped and again each group sent to a separate node for the second stage before the displaying.

3.3 The Multi-Node Cluster

The multi-node cluster developed for the beamforming process is built of a series of commodity personal computers (PCs) connected via a Myrinet high speed fiber-optic network for data transfer. An Ethernet network is also used for control messages [6,9]. The layout and interconnections of the components of this computing cluster is shown in Figure 5. The data acquisition unit delivers the acquired data to the PCI bus of the individual nodes as shown in Figure 5.
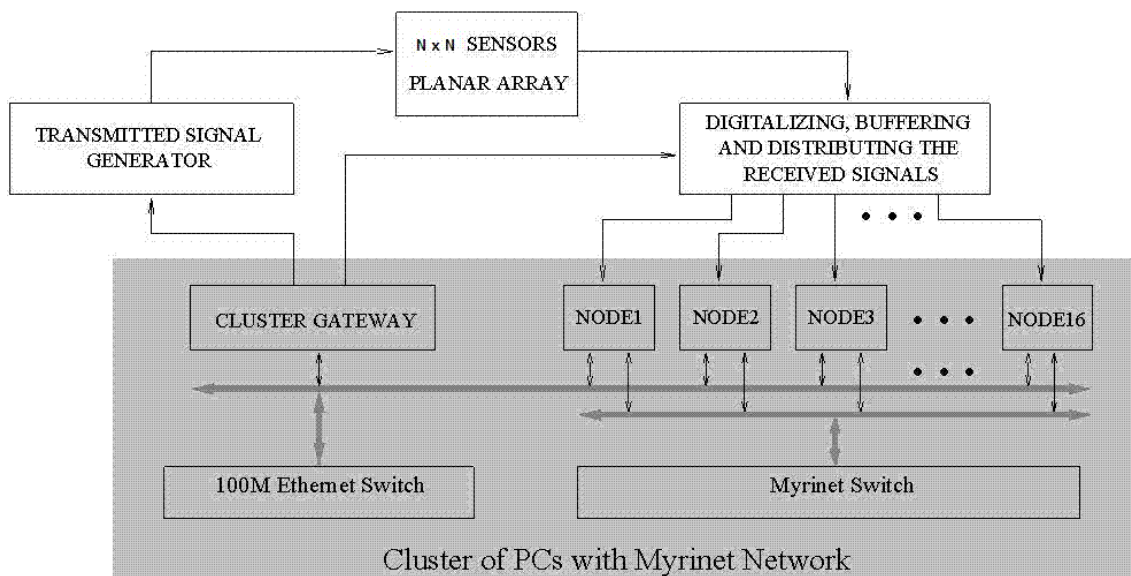
Figure 5: Layout of the computing cluster.

3.4 Computing Architecture and Implementation Issues

Implementation of a fully digital 3D adaptive beamforming structure in ultrasound systems is a non-trivial issue. In addition to the selection of the appropriate algorithms, success is heavily dependent on the availability of suitable computing architectures.

Past attempts to implement matrix based signal processing methods, such as adaptive beamformers, were based on the development of systolic array hardware because systolic arrays allow large amounts of parallel computation to be performed efficiently since communications occur locally. None of these ideas are new. Unfortunately systolic arrays have been much less successful in practice than in theory. The fixed size problem for which it makes sense to build a specific array is rare. Systolic arrays big enough for real problems cannot fit on one board, much less one chip, and interconnects have problems. A 2-D systolic array implementation will be even more difficult. So, any new computing architecture development should provide high throughput for vector as well as matrix based processing schemes.

A fundamental question, however, that must be addressed at this point is whether it is worthwhile to attempt to develop a dedicated architecture that can compete with a multiprocessor using stock microprocessors. However, the experience gained from sonar computing architecture developments [4] suggests that a cost effective approach in that direction is to develop a PC-based computing architecture that will be based on the

rapidly evolving microprocessor technology of the CPUs of PCs. Moreover, the signal processing flow of advanced processing schemes that include both scalar and vector operations should be very well defined in order to address practical implementation issues. When the signal processing flow is well established, such as in Figures 4 and 5, then distribution of the signal processing flow in a number of parallel CPU's will be straightforward. In the following sections, we address the practical implementation issues by describing the current effort of developing an experimental fully digital 3D/4D ultrasound system deploying a planar array to address the requirements of the Canadian Forces for non-invasive portable diagnostic devices deployable in fields of operations.

3.5   Technological Challenges for Fully Digital Ultrasound System Architecture

The current state-of-the-art in high-resolution, digital, 3D ultrasound medical imaging faces two main challenges:

First, the ultrasound signal processing structures are computationally demanding. Traditionally, specialized computing architectures and hardware have been used to provide the levels of performance *and* I/O throughput required, resulting in high system design and ownership costs. With the emergence of high-end workstations and low-latency, highbandwidth interconnects [9], it now becomes interesting and timely to investigate if such technologies can be used in building low-cost, high-resolution, 3D ultrasound medical imaging systems.

Second, although beamforming algorithms in digital configuration have been studied in the context of other applications [4,6], little is known about their computational characteristics with respect to ultrasound-related processing, and medical applications in general. It is not clear which parts of these algorithms are the most demanding in terms of processing or communication and how exactly they can be mapped on modern parallel PC-based architectures. In particular, although the algorithmic complexity of different sections can be calculated, little has been done in terms of actual performance analysis on real systems. The lack of such knowledge inhibits further progress in this area, since it is not clear how these algorithms should evolve to lead to applicable solutions in the area of ultrasound medical imaging.

The previous sections of this paper addresses both these two issues by introducing a design of a parallel implementation of the advanced 3D beamforming algorithms of [9] and studying its behavior and requirements on a generic computing architecture that consists of commodity components.

This design concept provides an efficient, all-software, sequential implementation that shows considerable advantages over hardware-based implementation of the past. It provides also an efficient parallel implementation of the advanced 3D beamforming of [6] for a cluster of high-end PCs connected with a lowlatency, high-bandwidth interconnection network that allows also for an analysis of its behaviour [9]. The emphasis in this design has been placed also on the identification of parameters that critically affect both the performance and cost of ultrasound system.

The end result reveals a number of interesting characteristics leading to conclusions about the prospect of using commodity architectures for performing all related processing in ultrasound imaging medical applications. A brief summary of these findings suggests the following:

- A PC-based 16-processor system today can achieve close-to-real-time performance for high-end ultrasound image quality and is certainly expected to do so in the near future [9].

- The major components of the digital 3D ultrasound beamforming signal processing structure of [9] that are very computationally intensive consist of:

- 85-98% of the time is spent in FFT and beam steering functions.

- The communication requirements in the particular implementation are fairly small, localized, and certainly within the capabilities of modern low-latency, high-bandwidth interconnects.

- The results of this section provide an indication of the amount of processing required for a given level of ultrasound image quality and number of channels in a probe and can be used as a reference in designing computing architectures for ultrasound systems.

4.0   EXPERIMENTAL RESULTS

4.1   System Overview

The experimental configuration of the fully digital ultrasound imaging concept included two versions. The first was configured to be integrated with a linear phase array ultrasound probe and it is depicted in Figure 6. This is a fully digital ultrasound system which includes the linear array probe (64 elements) and the 2-node data acquisition unit including two Mini-PCs that control the transmitting and receiving functions. This linear array ultrasound system was configured also to provide 3D images through volume rendering of the B-scan outputs as defined in [5]. A USB communication protocol allowed the transfer of the B-scans (2D digital images) as inputs to the visualization software for 3D volume rendering [5] installed in the portable PC. More specifically, the experimental linear array ultrasound system can provide 3D volumetric images from a series of B-scan (2D) outputs. The magnetic tracker system, provides the co-ordinates of the probe for each of the acquired image frames (B-scans). This tracker provides translational (x, y and z) as well as rotational co-ordinates with respect to the x, y and z, axes.
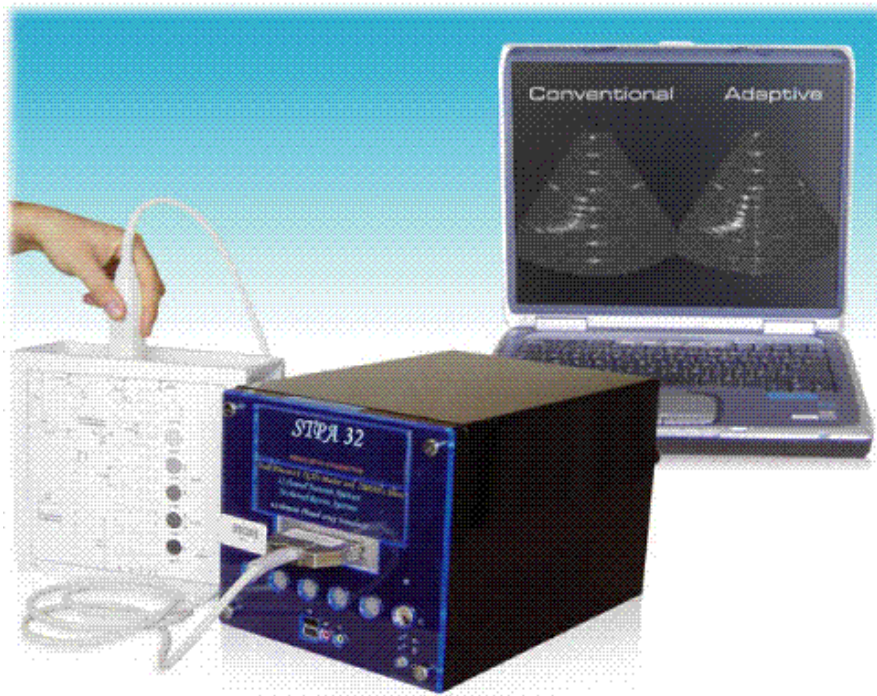

Figure 6: The experimental linear phase array (64-element) ultrasound imaging system integrated with a Laptop computer to provide visualization functionalities.

The second configuration is a fully digital planar phase array volumetric ultrasound imaging system, depicted in Figure 7. The multi-node computing cluster that allows for an effective implementation of the 3D beamforming structure is shown at the lower part of this figure. The top left image in Figure 7 shows the planar phase array probe and the top right image presents the data acquisition unit with the A/D and D/A peripherals controlled by the multi-node cluster.

Implementation of the 3D beamforming structure and communication requirements relevant with the system configuration of Figure 7, have been discussed already in the previous sections.

Figure 8 shows a schematic representation of the main components of the fully digital real time planar array ultrasound imaging system that summarizes the developments that have been presented in the previous sections. It depicts a 256: (16x16) element phased array probe, a A/DC with 64 channel data acquisition unit that through multiplexing acquires time series signals for the 256 channels, and a computing architecture to process the acquired time series into ultrasound volumes, shown also in Figure 7. In addition the system uses a 36-channel digital to analog converter (D/AC) to excite the center (6x6) transducers of the planar array during the illumination process. The transmit functionality that address the pulse design to illuminate at various depths simultaneously is addressed in a subsequent section. The inter-element spacing of the probe is 0.4mm in both directions. This combination forms the front end of the 3-D ultrasound system that will support the transmit functions and the receiving functions required for the 3-D beamforming. The probe is attached to the data acquisition unit via an interface card. This card provides the means of data flow into and out of the probe through the data acquisition system.

The computing cluster (Figure 7) that implements the 3D beamformer software (Figure 8) has already been introduced in the previous section. This is the multi-node cluster that was designed to allow for easy implementation of the 3-D beamformer algorithms – both conventional and adaptive. The integrated hardware platform in Figure 7 brings together the planar array probe, the data acquisition unit for the planar array probe and the multi-node PC cluster.
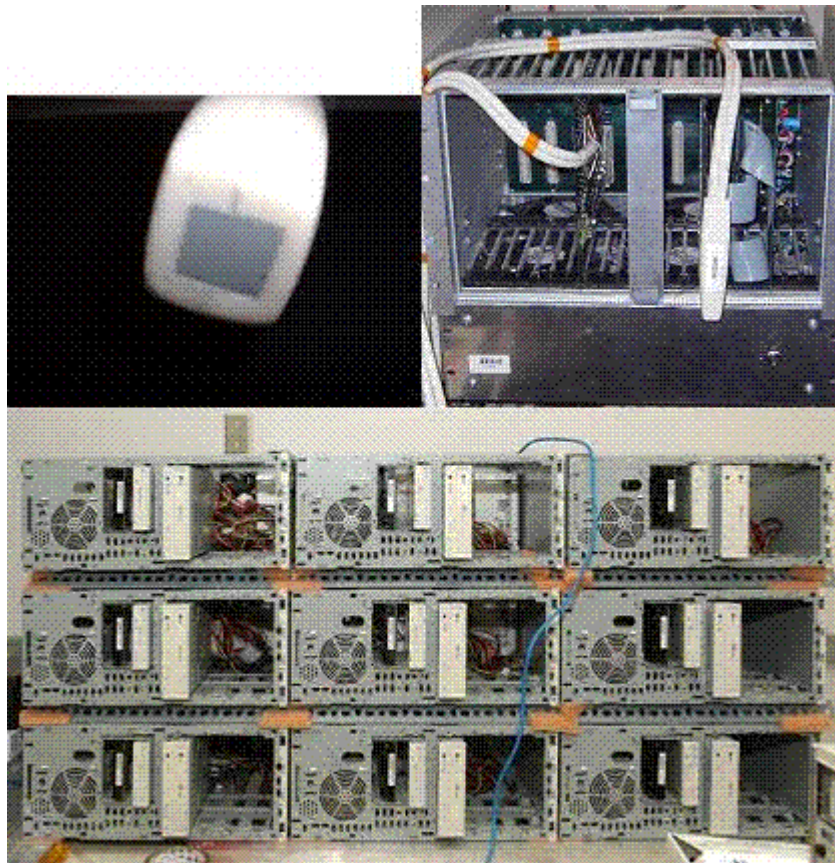
**Figure 7: The multi-node computing cluster that allows the implementation of the parallel beamforming
structure of the experimental planar phase array ultrasound imaging system is shown at the
lower part of this figure. The top left image shows the planar phase array probe and
the top right image depicts the data acquisition unit with the A/D and D/A
peripherals (with probe attached) controlled by the multi-node cluster.**

The A/DC is well grounded and capable to sample the 64 channels with an equivalent 14-bit resolution and 33 MHz sampling frequency per channel. Moreover, the unit has dedicated memory and separate bus-lines. The D/AC is capable to drive 36 channels with 12-bit resolution and 33 MHz sampling frequency. The period between two consecutive active transmissions is in the range of 0.2 ms. Moreover, the local memory of the D/AC unit has the capability to store the active beam time series with total memory size of 1.35 Mb, being generated by the main computing architecture for each focus depth and transferred to the local D/AC memory when the transmission-acquisition process begins.

The digitization process of the 16x4 sub-apertures by the 14-bit 64-channel A/D unit, provide the signals to a system of pin connectors-cables with suppressed cross-talk characteristics (minimum 35 dB). The sampling frequency is 33 MHz for each of the channels associated with a receiving single sensor. The multiplexer associated with the A/DC allows the sampling of the 16x4-sensors of the planar array in four consecutive active transmissions to be able to digitize the 16x16 planar array channels.
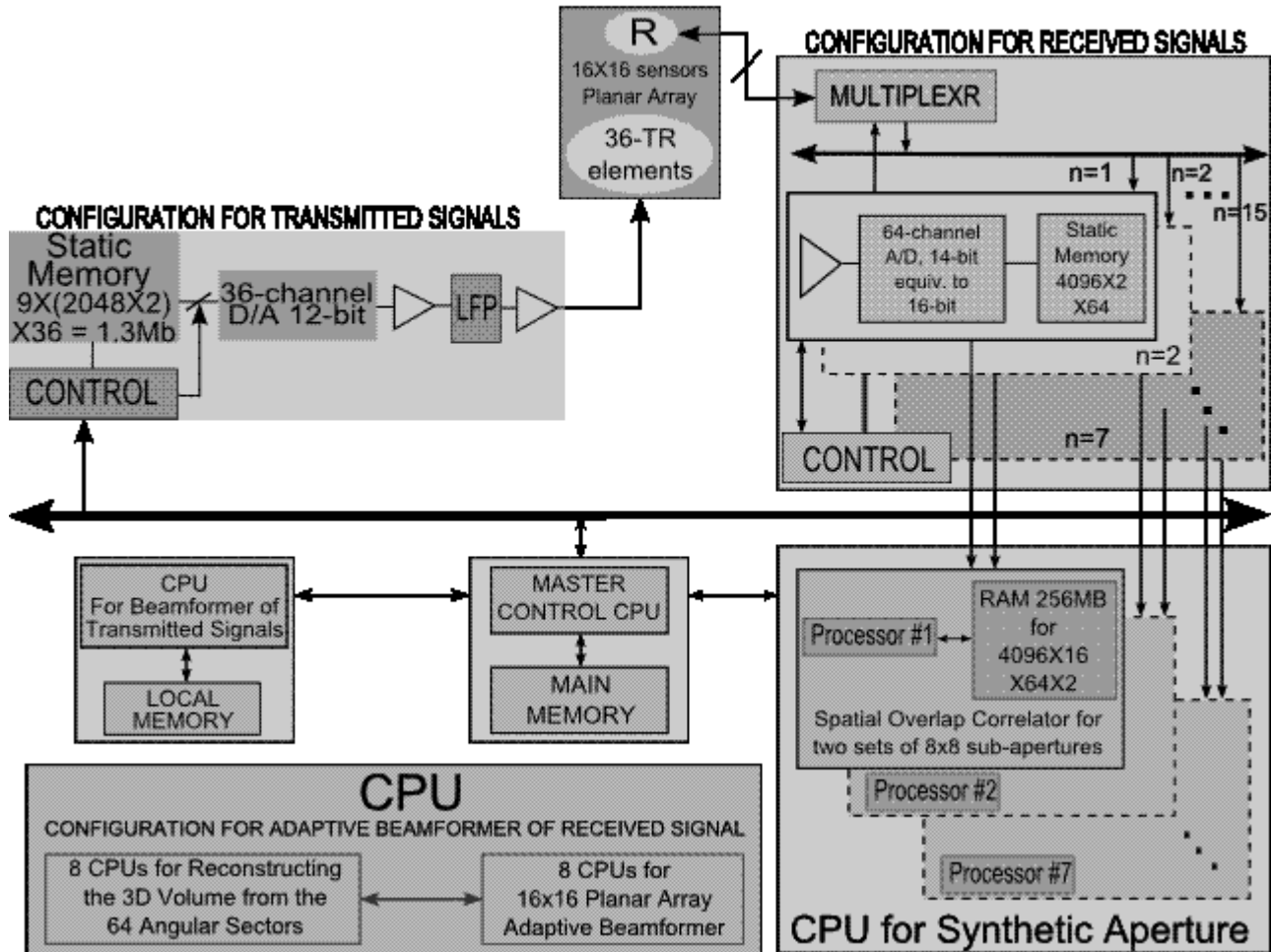
**Figure 8: Structure of the PC-based computing schematic representation of the main
components including the data acquisition units of a fully digital
real time planar array ultrasound imaging system.**

The computing architecture, (Figure 8), includes sufficient data storage capabilities for the sensor time series. The A/DC and signal conditioning modules of the data acquisition process and the communication interface are controlled through S/W drivers that form an integral part of the computing architecture.

It has been assessed that the ultrasound adaptive 3D beamforming structure, defined in [3], provides an effective beam-width size, which is equivalent to that of a two to three times longer aperture along azimuth and elevation of the deployed planar array. Thus, for the deployed receiving 16x16 planar array, the adaptive beamformer's beamwidth characteristics will be equivalent with those of a (16x2)x(16x2) size planar array. For example, the beam-width of a receiving 16x16 planar array with element spacing of 0.5 mm for a 3 MHz centre frequency, is approximately 7.4^{o}, with effective angular resolution by the adaptive beamformer in terms of beam-width size, to be less than **$3.7^{o} \times 3.7^{o}$.** As a result, the receiving adaptive beams along azimuth will have the following image resolution capabilities:

- **For C-scan** and for **depth of 10 cm**, the 3.7° x 3.7° angular resolution sector corresponds to a (0.64 cm) x (0.64 cm) = **0.41 cm^2 size of tissue resolution**, or for **depth of 5 cm** to a (0.32 cm) x (0.32 cm) = **0.10 cm^2 size of tissue resolution.**

- **For B-scan** the **line resolution** will be equivalent to the wavelength of the transmitted centre frequency , which is **0.5 mm**.

- Thus, the **volume resolution** of the 3D adaptive beamforming structure will be equivalent to (10.2 mm^2) x (0.5 mm) = **5.12 mm^3, in 3D tissue size at a depth of 5 cm.**

The concept of the energy transmission module to illuminate the entire volume of interest with a few firings, has been introduced in [6] and depicted in Figure 2. Here the volume is illuminated in sub-sectors. The transmitted signals are all broadband FM (chirp) signals. They are fired with inter-element delays to allow the transmitted energy to be focused at specific regions in space, (e.g. the space highlighted by the square shaded areas of Figure 2). The energy transmission is done through the 6 x 6 elements at the center of the array. The transmit patterns are loaded into the memory of the data acquisition unit and delivered to the probe via the D/AC portion of the unit when a trigger signal is received. In addition, FM pulses that occupy different non-overlapping frequency regimes may be coded together to illuminate different focal depths with a single firing. This means that it can be arranged so that one frequency regime can focus and illuminate the lower shaded square, and a second frequency regime the upper shaded square in Figure 2.

Suppose three focal depths $d_1 < d_2 < d_3$ are desired. Then, three separate sets of transmit patterns are created. The first set of transmit patterns with the appropriate delay profiles that occupy the lowest frequency band are designed to focus at depth d_3. A second set of transmit patterns with delay profiles to focus at depth d_2 are designed to occupy a second frequency band higher than the first and with no frequency overlap. Similarly, a third set of transmit patterns are designed to focus at focal depth d_1. This third set of patterns is designed to occupy the highest frequency band since they will illuminate the shallow regions of the medium of interest. When the design of the three sets of transmit patterns is complete they are superimposed to create a single transmit pattern. This composite transmit pattern is used to provide the illumination as described in Figure 2. However, the requirement to use the smallest possible number of illumination beams leads to a non-uniform energy distribution in space. This requires the application of a linearization function to correct for this type of non-uniformity. A correction function is derived from the illuminating beam shapes and is used later for linearization of the results of the beamformer. An example of a linearization function is shown in Figure 4. This figure shows the correction function that would be applied to the output of a 4 x 4 sub-sector illuminations.

4.2   Performance Results

Presented in this section are the image output results from the linear phase array (e.g. 64-elements, 2D/3D) and the planar phase array probes (e.g. 16x16, 3D/4D). While numerous experiments were carried out, only a few typical image/volume outputs for both the adaptive and conventional image results are presented here. All these image results are from the standard ultrasound "test target" termed as phantom, the cross section of which is shown in Figure 28.
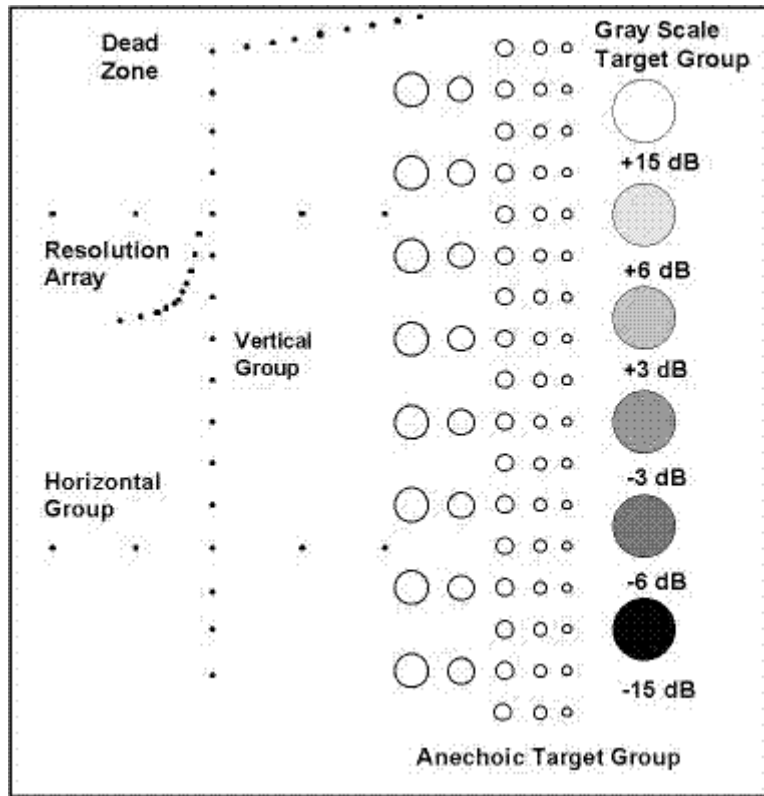
Figure 9: Cross sectional view of the experimental phantom.

4.3   Portable 2D/3D Experimental System with Linear Phased Array Probe

4.3.1   B-Scan Results

Figure 10 shows two typical images from the portable 2D/3D system operating in B-scan mode. The left hand image shows the image obtained using the conventional beamforming technique and the right hand image shows the image output from the adaptive beamformer. Both images are obtained by placing the probe on the top of the phantom just above the "Dead Zone" label. The phantom's vertical row of reflectors and the curved arrangement are depicted in both images that show no "ghosting" or blurring of these strong reflectors.

The next figure 11 provides a comparison of the B-scan outputs from a commercial ultrasound imaging system and the experimental prototype of this investigation depicted in Figure 6. The images for both systems are obtained by placing the probes on the left side of the phantom just beside the "Resolution Array" label. Both systems use the same probe (64-channels). However, the commercial system operates at 4 MHz while the experimental system in Figure 6 operates at 2 MHz. The left hand side image (Figure 11a) shows the output of the adaptive beamformer at 2 MHz while Figure 11b shows the image output from the commercial 4 MHz ultrasound system.
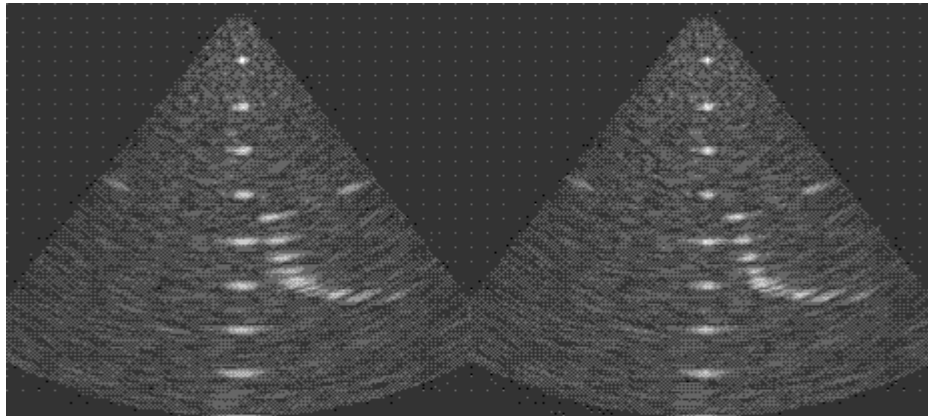
Figure 10: B-scan image results for both the Conventional (Left Hand Side Image) and Adaptive (Right Hand Side Image) beamformers of the experimental linear phase array (64-element) ultrasound imaging system, depicted in Figure 6.
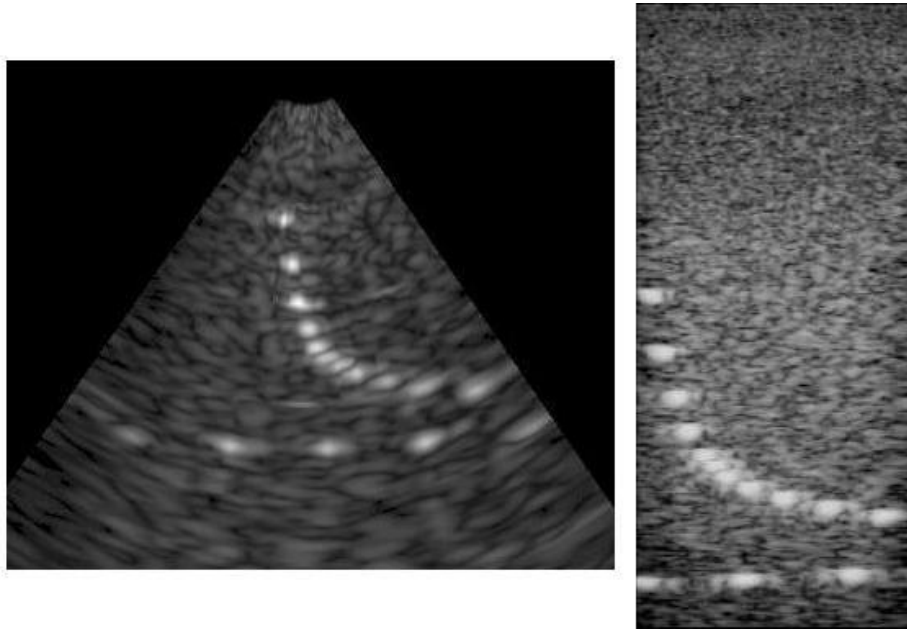

Figure 11: The left hand side image (30a) shows the B-scan output of the adaptive beamformer for the same phantom as in Figure 29, illuminated at 2 MHz. The right hand side image (30b) shows the output of a commercial system using the same probe at 4 MHz.

It can be seen from the image results of Figure 11 that the adaptive beamforming scheme of this investigation performs quite as good, if not even better, with respect to the ultrasound commercial system, in terms of both resolution of the strong scatterers, and noise in the bulk image. It should furthermore be considered that the images obtained with the prototype of this investigation have been acquired using a 2MHz probe, whereas a 4MHz probe has been employed for the image output (Figure 11b) of the commercial system.

The transmission/acquisition schemes adopted by the experimental 2D/3D prototype system allow to cover a wide scanning angle (90°-120°), a characteristic which can be very useful in cardiac imaging applications.

Furthermore, the deployment of low frequencies in the range of 2 MHz can achieve the deep penetration depths which are required in cardiologic ultrasound applications.

4.3.2   Volumetric 2D/3D Imaging

The volumetric images created from the 2D/3D system are shown in Figure 12. This figure shows cross sections of the 3D output from volume redering of B-scan images using the techniques discussed in [5]. In particular, Figure 11 shows the volume obtained using the standard ultrasound phantom of Figure 9. In this experiment the volume is taken along the top surface of the phantom. The top right panel in Figures 12 shows the full reconstructed volume. The remaining 3 panels show three orthogonal views of the volume scanned. The visualization software is discussed in [5].

Although the experimental 2D/3D system in Figure 6 includes a fully digital ultrasound technology with an advanced beamforming structure implemented in frequency domain, this system has been reduced to a portable size, compared to nowadays commercial ultrasound units.
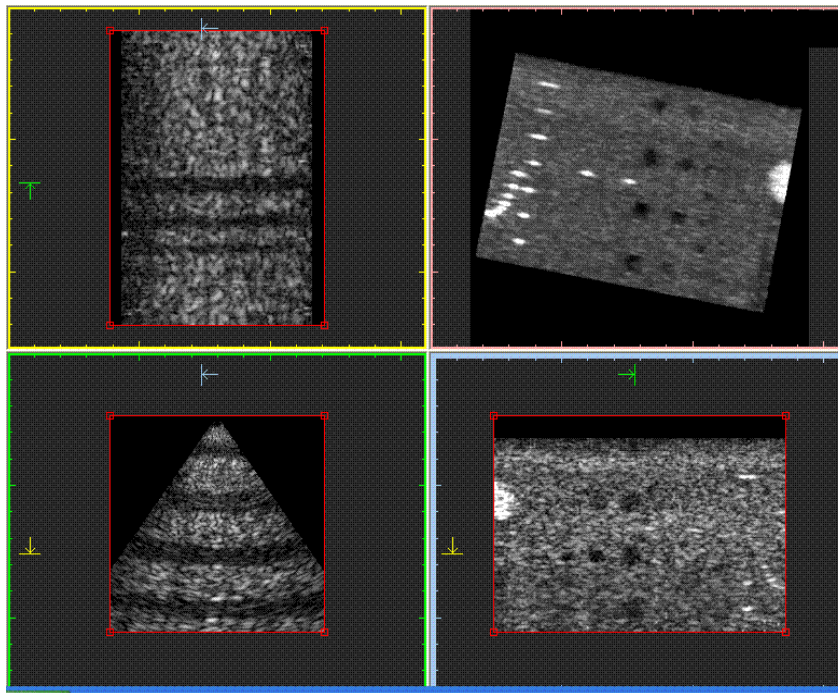

**Figure 12: The 3D volume is taken along the top surface of the phantom shown in Figure 28.
The top right panel shows the full reconstructed volume. The remaining
3 panels show three orthogonal views of the volume scanned.**

4.3.3   3D/4D Experimental System with Planar Phase Array Probe

The volumes created from the 3D/4D system, deploying the planar (16x16) phase array probe, are shown in Figures 13 and 14. Figure 13 shows the volume derived from the 3D conventional beamformer and Figure 14 presents the output of the 3D adaptive beamformer. The volumes in both figures are obtained by placing the probe on the left side of the phantom just beside the "Resolution Array" label. The top right panel in Figures

32 and 33 show the full reconstructed volume in each case. The remaining 3 panels show three orthogonal views of the volume scanned.

Like the portable ultrasound 2D/3D unit, the experimental 3D/4D system deploying a planar phase array probe has the capability of performing both conventional as well as adaptive beamforming, and both the modules are integrated into the parallel processing scheme discussed in this report. Furthermore, the 3D/4D system is also capable of frequency coding for multi-zone focusing, and of applying deblurring algorithms for enhancing the image quality. Both experimental systems (e.g. 2D/3D, 3D/4D) show good performances in terms of scanning angle apertures, penetration depth and image quality. As expected, the adaptive beamforming scheme implemented into the 3D parallel architecture seems to allow for a higher image quality with respect to conventional beamforming for what concerns the axial and contrast resolutions.
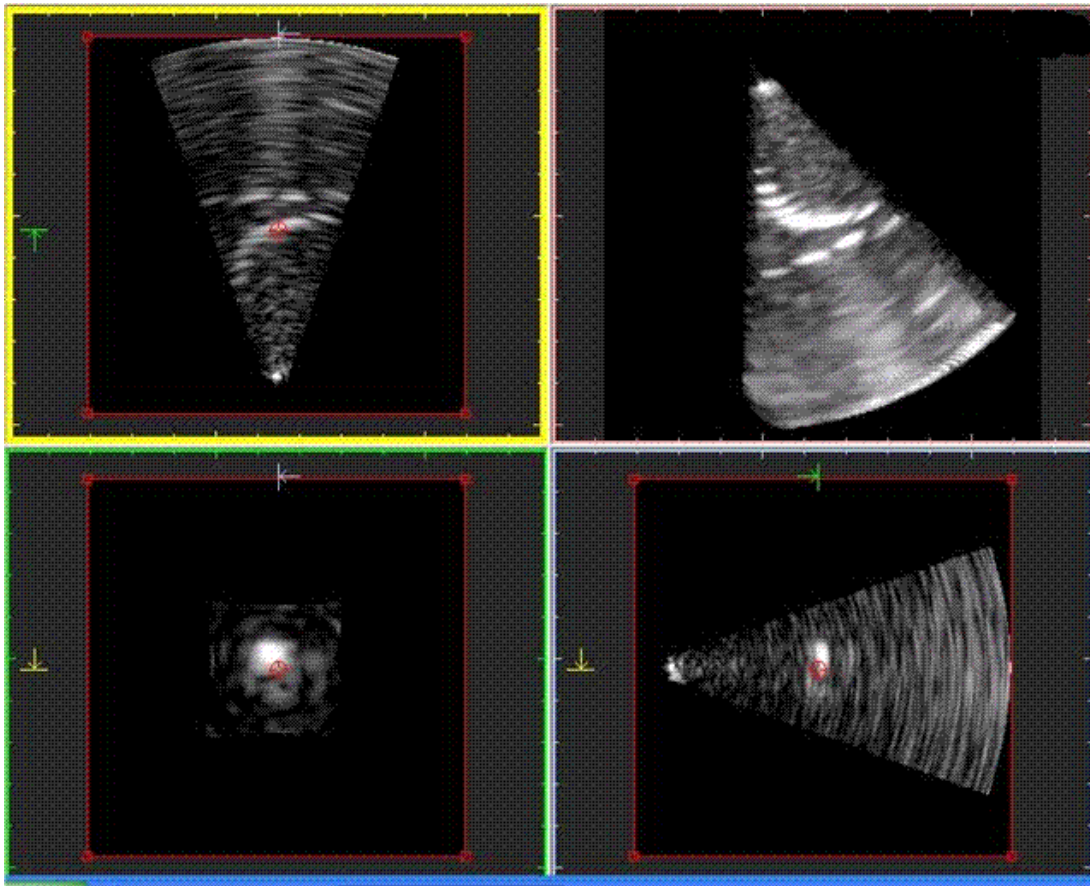

Figure 13: Reconstructed 3D volume from the beam time series of the 3D conventional beamformer. The top right panel shows the full reconstructed volume. The remaining 3 panels show three orthogonal views of the volume scanned.
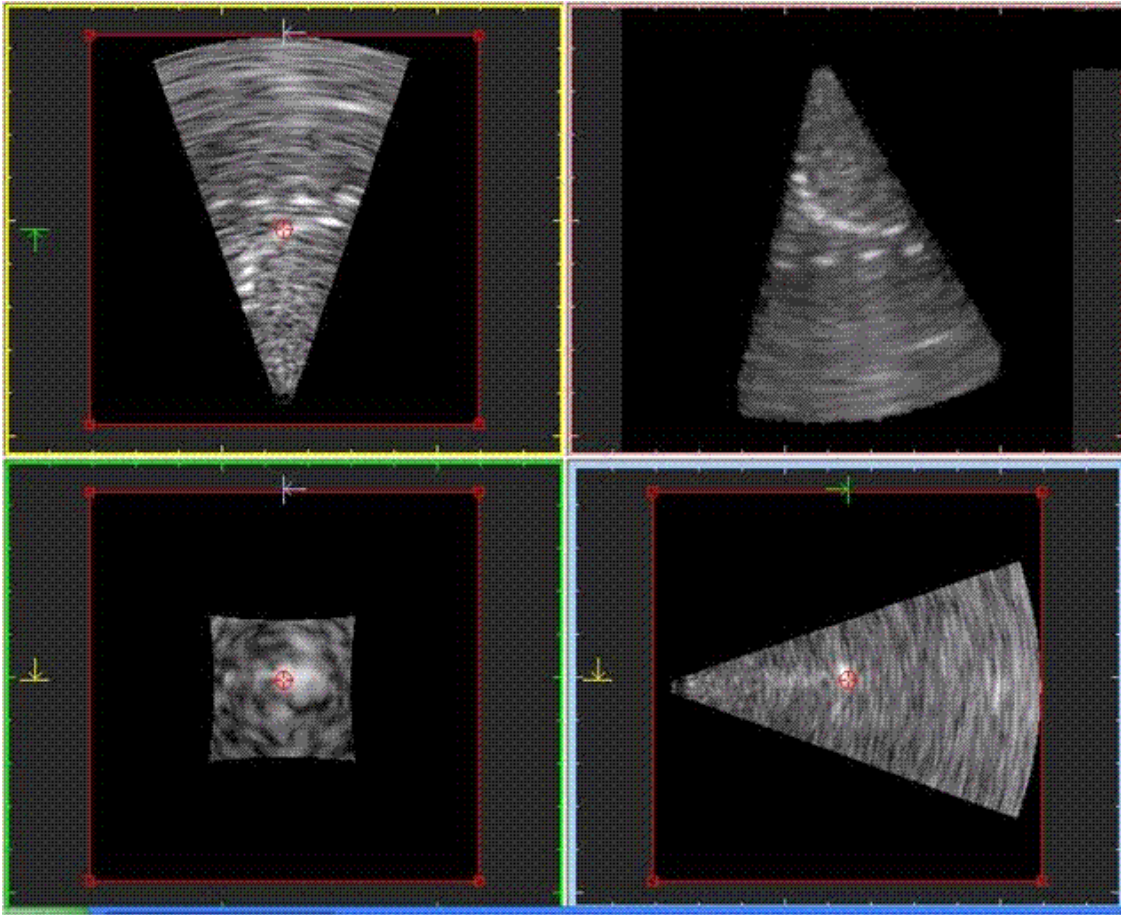
Figure 14: Reconstructed 3D volume from the beam time series of the 3D adaptive beamformer. The volumes in both figures 13 and 14 are obtained by placing the probe on the left side of the phantom just beside the "Resolution Array" label. The top right panel shows the full reconstructed volume. The remaining 3 panels show three orthogonal views of the volume scanned.

5.0   CONCLUSION

The fully digital ultrasound system technology discussed in this paper consists of a set of unique adaptive ultrasound beamformers [1,2,3], a PC-based computing architecture and a set of visualization tools, presented in [3,6,9], addressing the fundamental image resolution problems of current 3D ultrasound systems. The results of this development can be integrated into existing 2D and/or 3D ultrasound systems or they can be used to develop a complete stand-alone 3D ultrasound system solution.

It has been well established [6] that the existing limitations of medical ultrasound imaging systems in poor image resolution, is the result of the very small size of deployed arrays of sensors and the distortion effects by the influence of the human-body's non-linear propagation characteristics. The ultrasound technology, discussed in this paper, replaces the conventional (time delay) beamforming structure of ultrasound systems with an adaptive beamforming processing configuration that has been developed for sonar array systems. The results of this development [1-3,6-8] have demonstrated that these novel adaptive beamformers improve significantly (at very low cost) the image resolution capabilities of an ultrasound imaging system by providing

a performance improvement equivalent to a deployed ultrasound probe with double aperture size . Furthermore, the portability and the low cost for the 3D ultrasound systems offer the options to medical practitioners and family physicians to have access of diagnostic imaging systems readily available on a daily basis.

At this point, however, it is important to note that in order to fully exploit the advantages of this digital adaptive ultrasound technology, its implementation in a commercial ultrasound system requires that the system has a fully digital design configuration consisting of A/DC and D/AC peripherals that would fully digitize the ultrasound probe time series, they will optimally shape the transmitted ultrasound pulses through a D/A peripheral and they will use phase array linear or matrix ultrasound probes.

In other words, the present ultrasound technological alternative, revises the signal processing configuration of ultrasound devices and moves it away from the traditional hardware and implementation software requirements.

Thus, implementation of the adaptive beamformer is a software installation on a PC-based ultrasound computing architecture with sufficient throughput for 3D and 4D ultrasound image processing. As a result, the ultrasound computing architecture, discussed in this report, is able to accommodate the processing requirements of the "traditional" linear array 2D scans as well as the advanced matrix-arrays performing volumetric scans.

In addition, the use of adaptive ultrasound beamformers, provides significantly better image resolution than the traditional time delay based beamformers. Thus, a good image resolution can be achieved with less aperture size and sensors, thus decreasing the hardware costs of an ultrasound system.

In summary, the PC-based ultrasound computing architecture of this report, its adaptive 2D & 3D ultrasound beamforming structure and the set of visualisation tools allow for a flexible cost-to-image quality adjustment. The resulting product can be upgraded on a continuous base at very low cost by means of software improvements and by means of hardware by taking advantage of the continuous upgrades and CPU performance improvements of the PC-based architectures. Thus, for a specific image resolution performance, a complete re-design or product upgrade can be achieved by means of software improvement, since the digital hardware configuration would remain the same.

REFERENCES

[1] Stergios Stergiopoulos and Amar Dhanantwari, "High Resolution 3D Ultrasound Imaging System Deploying a Multi-Dimensional Array of Sensors and Method for Multi-Dimensional Beamforming Sensor Signals" Assignee: Defence R&D Canada, US Patent: 6,482,160, issued 19 Nov. 2002.

[2] Stergios Stergiopoulos and Amar Dhanantwari, "High Resolution 3D Ultrasound Imaging System Deploying a Multi-Dimensional Array of Sensors and Method for Multi-Dimensional Beamforming Sensor Signals" Assignee: Defence R&D Canada, US Patent: 6,719,696, issued 13 April 2004.

[3] S. Stergiopoulos, "Advanced Beamformers", Chapter in 2nd Edition, Handbook on Advanced Signal Processing for Sonar, Radar and Non-Invasive Medical Diagnostic Systems, Editor: S. Stergiopoulos, CRC Press LLC, Boca Raton, FL, USA, pg: 79-146, March 2009.

[4] Stergiopoulos S., "Implementation of Adaptive and Synthetic Aperture Beamformers in Sonar Systems", *Proc. of the IEEE* , **86**(2), 358-396, Feb. 1998.

[5]   Sakas G., Karangelis G., Pommert A., "Advanced Applications of Volume Visualisation Methods in Medicine", Chapter in 2nd Edition, Handbook on Advanced Signal Processing for Sonar, Radar and Non-Invasive Medical Diagnostic Systems, Editor: S. Stergiopoulos, CRC Press LLC, Boca Raton, FL, USA, March 2009.

[6]   S. Stergiopoulos, "Digital Ultrasound 3D/4D Imaging Technology", Chapter in 2nd Edition, Handbook on Advanced Signal Processing for Sonar, Radar and Non-Invasive Medical Diagnostic Systems, Editor: S. Stergiopoulos, CRC Press LLC, Boca Raton, FL, USA, pg: 457-498, March 2009.

[7]   A. Dhanantwari, S. Stergiopoulos, C. Parodi, F. Bertora, P. Pellegretti, A. Questa, "An efficient 3D beamformer implementation for real-time 4D ultrasound systems deploying planar array probes", Proceedinds of the IEEE UFFC'04 Symposium, Montreal, Canada, August 2004

[8]   A. Dhanantwari, S. Stergiopoulos, C. Parodi, F. Bertora, A. Questa and P. Pellegretti, " Adaptive 3D Beamforming for Ultrasound Systems Deploying Linear and Planar Array Phased Array Probes", IEEE Conference Proceedings, IEEE International Ultrasonics Symposium, Honolulu Hawaii, Oct. 5-8, 2003.

[9]   F. Zhang, A. Bilas, A. Dhanantwari, K.N. Plataniotis, R. Abiprojo and S. Stergiopoulos. "Parallelization and Performance of 3D Ultrasound Imaging Beamforming Algorithms on Modern Clusters". Proceedings of the 16th International Conference on Supercomputing (ICS'02), New York, June 2002.